AJNR

CT and MR Imaging Findings of Periorbital Lipogranuloma Developing after Endoscopic Sinus Surgery

B.T. Yang, Y.J. Liu, Y.Z. Wang, X.Y. Wang and Z.C. Wang

AJNR Am J Neuroradiol published online 21 June 2012
http://www.ajnr.org/content/early/2012/06/21/ajnr.A3182

Published June 21, 2012 as 10.3174/ajnr.A3182

CLINICAL REPORT

CT and MR Imaging Findings of Periorbital Lipogranuloma Developing after Endoscopic Sinus Surgery

B.T. Yang
Y.J. Liu
Y.Z. Wang
X.Y. Wang
Z.C. Wang

SUMMARY: Periorbital lipogranuloma is a rare complication after ESS and presently lacks specific imaging reports. The purpose of this study was to describe the CT and MR imaging features of periorbital lipogranuloma. We retrospectively reviewed 9 patients with histology-confirmed periorbital lipogranuloma. All 9 patients underwent CT and MR imaging. Five lipogranulomas were located in the right eyelid and 4 in the left eyelid, which extended into the extraconal space to some degree. The lesions displayed an irregular shape and had an ill-defined margin. Multiple, specked, or nodular foci containing fat were scattered within these lesions. The lesions demonstrated moderate heterogeneous contrast enhancement on contrast-enhanced MR imaging. The TICs showed a persistent pattern (type I) in 6 patients undergoing DCE MR imaging. Thus, an ill-defined, irregular-shaped periorbital mass with multiple foci containing fat, combined with an ESS history, can help to accurately diagnose this entity.

ABBREVIATIONS: DCE = dynamic contrast-enhanced; ESS = endoscopic sinus surgery; HU = Hounsfield units; TIC = time-intensity curve; Tpeak = time to peak enhancement; WR = washout ratio

ESS has become a widely accepted procedure for the treatment of sinonasal cavity disease. Although ESS is generally a safe surgical procedure, complications can occasionally occur, especially in the orbit due to the close proximity of the paranasal sinus. Even though orbital complication is <1%, some complications can result in serious morbidity, the most devastating of which is loss of vision.[1] The common orbital complications include lamina papyracea fracture, retrobulbar hematoma, extraocular muscle injury or entrapment, ocular dysmotility, orbital emphysema, nasolacrimal duct injury, and optic nerve damage.[2] In addition, an uncommon and previously unnoticed orbital complication, periorbital lipogranuloma, may occur.

In the literature, approximately 20 cases have been documented in which this complication has occurred after ESS.[3-8] However, its occurrence might be more frequent than is initially thought because some cases may have been incorrectly diagnosed as other entities. Currently, imaging studies play an important role in the evaluation of this entity; unfortunately, no specific imaging study was found until now. During the past 5 years, we have encountered 9 patients who developed typical periorbital lipogranuloma several weeks or months after ESS. Here, we comprehensively studied the CT and MR imaging findings of these 9 cases to enhance recognition of this rare complication after ESS.

Received February 7, 2012; accepted after revision March 5.

From the Department of Radiology (B.T.Y., Y.Z.W., X.Y.W., Z.C.W.), Beijing Tongren Hospital, Capital Medical University, Beijing, China; and Department of Radiology (Y.J.L.), Lingxian Hospital, Shandong Province, China.

B.T. Yang and Y.J. Liu are co-first authors.

This work was supported by grants from the Special Fund of Sanitation Elite Reconstruction of Beijing (2011-3-048) and from the Beijing Municipal Natural Science Foundation (7112030).

The work on this article was provided in the following manner: study concepts, B.T. Yang, Y.J. Liu; study design, B.T. Yang, Y.J. Liu; definition of intellectual content, B.T. Yang, Y.J. Liu; literature research, Y.Z. Wang, X.Y. Wang; clinical studies, B.T. Yang, Y.Z. Wang; data acquisition, B.T. Yang, Y.Z. Wang; data analysis, B.T. Yang, Y.Z. Wang, X.Y. Wang; manuscript preparation, B.T. Yang, X.Y. Wang; manuscript editing, B.T. Yang, Y.J. Liu; manuscript review, B.T. Yang; manuscript revision, B.T. Yang, Y.J. Liu, Z.C. Wang.

Please address correspondence to Ben Tao Yang, MD, Department of Radiology, Beijing Tongren Hospital, Capital Medical University, No. 1, Dongjiaominxiang, Dongcheng District, Beijing 100730, China; e-mail:cjr.yangbentao@vip.163.com

http://dx.doi.org/10.3174/ajnr.A3182

Materials and Methods

Patients

This study was approved by the institutional review board of Beijing Tongren Hospital. Nine patients with orbital lipogranulomas confirmed by histology during a 5-year period (August 2006 to October 2011) were retrospectively reviewed. This study included 5 females and 4 males, with an age range of 14–55 years and a mean age of 37 years at diagnosis. Seven patients underwent surgical removal of the lesions by using a subciliary approach, and biopsies were performed in the other 2 patients to make a definite diagnosis.

All 9 patients previously underwent surgical removal of sinonasal cavity lesions by ESS at outside hospitals. A review of the operative notes indicated that nasal packing with Vaseline gauze (Covidien, Mansfield, Massachusetts) soaked in mineral oil controlled bleeding during ESS in 3 patients. A bony breach of the lamina papyracea was noted in 5 patients. All patients who underwent ESS were seen several weeks or months afterward for eyelid masses at our ophthalmology clinics.

The clinical data, including those from ophthalmologic clinics, were extracted from the medical records. The clinical data are summarized in the Table.

CT Technique

Nonenhanced orbital CT was performed in all 9 patients. Images were obtained in both the axial and coronal planes in all 9 by using a LightSpeed 16-section CT scanner (GE Healthcare, Beijing, China) or a Brilliance 64-section CT scanner (Philips, Healthcare, Best, the Netherlands). The imaging parameters were as follows: voltage, 120

Clinical features of 9 patients with periorbital lipogranuloma following ESS

Patient No.	Sex/Age (yr)	LP Breach	VG Packing	Time from Surgery to Presentation (mo)	Symptoms and Signs	Treatment	Follow-Up (mo)
1	M/14	N	N	3	Eyelid swelling, painless mass	Surgery	8
2	F/25	Y	Y	5	Eyelid swelling, painless mass	Surgery	14
3	M/55	N	N	4	Eyelid swelling, painless mass	Surgery	10
4	M/52	Y	N	4	Eyelid swelling, painless mass	Surgery	6
5	F/27	N	Y	7	Eyelid swelling, painless mass	Steroids and antibiotics	18
6	F/38	Y	Y	3	Eyelid swelling, painless mass	Steroids and antibiotics	35
7	F/41	Y	N	2	Eyelid swelling, painless mass	Surgery	15
8	M/30	Y	N	1	Eyelid swelling, painless mass	Surgery	9
9	F/51	N	N	25	Eyelid swelling, painless mass	Surgery	11

Note:—LP indicates lamina papyracea; VG, Vaseline gauze; Y, yes; N, no.

Kv; current, 200 mA; matrix, 512 × 512; section thickness, 2 mm. These CT images were reconstructed by using both a soft-tissue algorithm (window width of 400 HU at a window level of 40 HU) and a bone algorithm (window width of 4000 HU at a window level of 700 HU). Reformations were performed from the superior margin to the inferior margin of the orbit on the axial plane and from the anterior margin of the orbit to the anterior clinoid process on the coronal plane.

MR Imaging Technique

All 9 patients underwent orbit MR imaging before surgery or biopsy. The MR imaging examinations were performed on a 1.5T MR imaging system (GE Healthcare, Milwaukee, Wisconsin) with an 8-channel head coil. Fast spin-echo pulse sequences were used in these patients. They underwent pre-enhanced T1WI and T2WI and postenhanced T1WI in the axial, coronal, and sagittal planes. Postcontrast T1WI with frequency-selective fat saturation was obtained in the axial or coronal plane that optimally showed the lesion. The imaging parameters were as follows: T1WI: TR, 500–600 ms; TE, 10–15 ms; T2WI: TR, 3500–4000 ms; TE, 120–130 ms; NEX, 2–4; echo-train length, 11–27; matrix, 256 × 256; FOV, 18 × 18 cm; section thickness, 3 mm; intersection gap, 0.3 mm.

Gadopentetate dimeglumine (Magnevist; Bayer Schering, Berlin, Germany) was administered intravenously at a flow rate of 2 mL/s (total dose, 0.1 mmol per kilogram of body weight) by using a power injector (Medrad, Indianola, Pennsylvania) followed by a 10-mL flush of normal saline solution. DCE MR imaging was performed by using 3D fast-spoiled gradient recalled imaging before conventional postcontrast T1WI in 6 patients. The scan parameters were as follows: TR, 8.4 ms; TE, 4.0 ms; NEX, 1; matrix, 256 × 160; FOV, 18 × 18 cm; section thickness, 3 mm; intersection gap, 0 mm. A total of 12 sets of dynamic images were acquired. Each set included 6 images and required 13 seconds; the interset time gap was 12 seconds. The whole dynamic series took 5 minutes in total. After the dynamic scan, source images were transferred to an AW 4.4 workstation (GE Healthcare) for further analysis.

In the maximal section of the lesions, the authors manually drew regions of interest on the dynamic images for assessment of the enhancement kinetics of orbital lipogranulomas. The region of interest was approximately 3–4 mm in diameter. The area that showed the greatest degree of early enhancement was chosen; then, the corresponding TIC could be generated. At the same time, the change in signal intensity of a similar region of interest placed on the extraocular muscle was used for reference.

Image Analysis

The CT and MR images were interpreted in consensus by 3 authors (B.T.Y., Y.Z.W., and X.Y.W.) with 14, 8, and 6 years of experience in head and neck MR imaging, respectively.

In the present study, we adopted the classification scheme of the TIC of DCE MR imaging proposed by Yabuuchi et al[9] and Hisatomi et al.[10] The TICs were analyzed qualitatively as 3 types: 1) type I (persistent pattern) appears as a straight or curved line, and enhancement continues during the entire dynamic study (Tpeak: >60 seconds); 2) type II (plateau pattern) appears as a growing enhancement in the early stage and then displays a sharp bend to form a plateau in the middle and later stages (Tpeak: ≤60 seconds, 10% ≤ WR ≤ 20%); and 3) type III (washout pattern) appears as rapid enhancement during the early stage and then a rapid decrease in the middle and later stages (Tpeak ≤60 seconds, WR >20%).

Results

All 9 patients presented with eyelid swelling with normal color of the covering skin. Ocular examination showed firm, ill-defined, and nontender masses in the eyelids. The mean time was 6 months (range, 1–25 months) from ESS to presentation with a palpable eyelid mass.

Histologically, the lesions typically exhibited inflammatory granulomas with numerous histocytes, multinucleated foreign-body giant cells, multiple rounded empty vacuoles consistent with fat, and a variably significant infiltrate of lymphocytes and plasma cells. Immunohistochemistry revealed positivity for CD68.

All occurrences of periorbital lipogranulation were located at the eyelid, arising from the right eyelid in 5 patients (lower eyelid in 3 and upper eyelid in 2) and the left eyelid in 4 (lower eyelid in 3 and upper eyelid in 1), with extension into the extraconal space to some degree. The lesions gave rise to diffuse thickening of the affected eyelids, with an irregular shape and an ill-defined margin.

On nonenhanced CT, lipogranulomas appeared inhomogeneously isoattenuated to adjacent extraocular muscle with multiple locules of fat deposits (Fig 1*A*, -*B*). The lesions appeared heterogeneously isointense on both the T1- and T2-weighted images (Figs 2*A* and 3*A*, -*B*). Multiple, specked, or nodular well-defined areas that showed high signal on the T1-weighted imaging, intermediate signal on the T2-weighted imaging, and low signal on the fat-suppressed MR imaging corresponded to the fat droplets his-

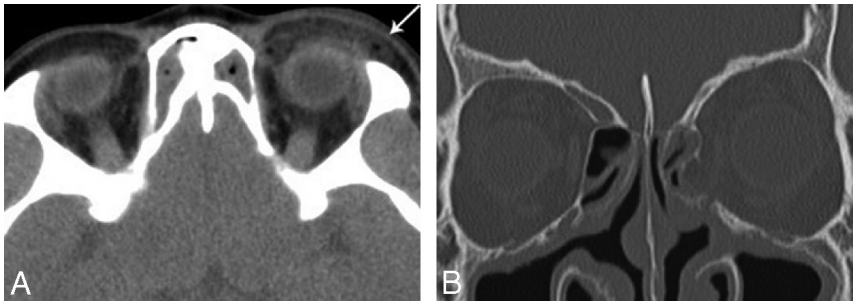

Fig 1. Case 2. *A*, Axial CT scan with a soft-tissue algorithm shows an irregular-shaped ill-defined mass in the left upper eyelid with multiple locules of fat deposits (*arrow*). *B*, Coronal CT scan with a bone algorithm shows the post-ESS appearance of the sinonasal cavity with fracture of the medial wall of the left orbit.

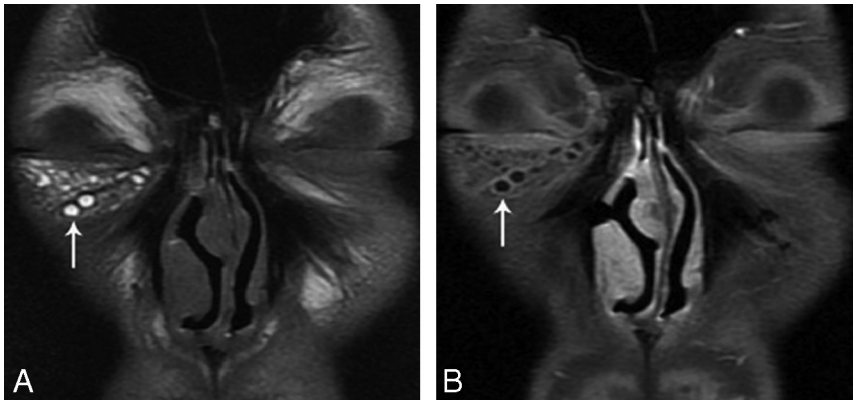

Fig 2. Case 1. *A*, Coronal T1-weighted image shows diffuse thickening of the right inferior eyelid with isointense signal intensity. Note multiple, speckled, and nodular high-signal foci within the lesion (*arrow*). *B*, Coronal contrast-enhanced T1-weighted image with fat saturation shows moderate inhomogeneous enhancement of the lesion. Note multiple low-signal foci (*arrow*) corresponding to high-signal foci seen on T1-weighted images within the lesion, which is consistent with fat.

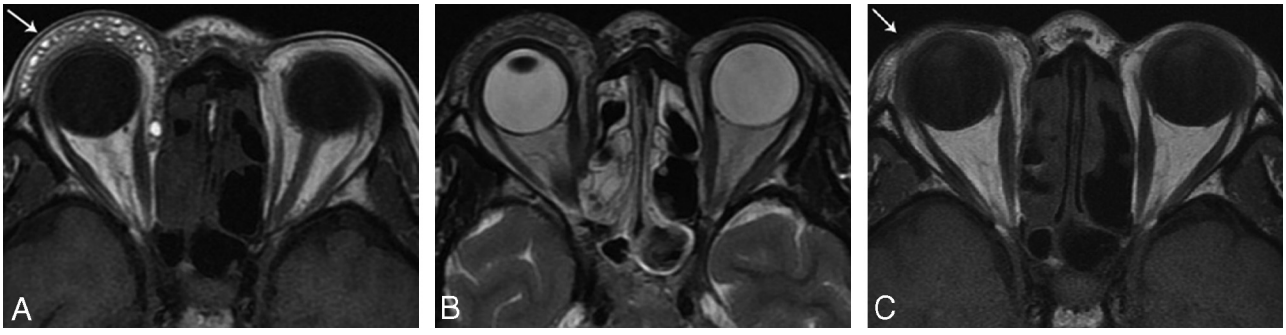

Fig 3. Case 5. *A*, Axial T1-weighted image shows an irregular-shaped, ill-defined, and heterogeneous isointense soft-tissue mass arising from the right upper eyelid, extending into the extraconal space (*arrow*). Note multiple, speckled, and nodular high-signal foci within the lesion. *B*, On the axial T2-weighted image, the lesion has heterogeneous isointense signal intensity with scattered intermediate signal foci corresponding to those foci identified on T1-weighted images. *C*, On the axial T1-weighted image, the lesion was resolved at 12-month follow-up after biopsy (*arrow*).

tologically (Figs 2*A*, -*B* and 3*A*, -*B*). The lesions typically demonstrated moderate heterogeneous enhancement on conventional contrast-enhanced images following the administration of contrast material (Fig 2*B*). Six patients (cases 1–6) underwent DCE MR imaging, and the TICs appeared as a persistent pattern (type I).

Other imaging findings related to periorbital lipogranuloma: 1) post-ESS appearances of the sinonasal cavity (Fig 1*B*), and 2) bony incontinuity of the medial wall of the orbit in 5 patients (Fig 1*B*).

All 9 patients were followed up for >6 months (mean, 14 months; range, 6–35 months). Seven patients who underwent surgical resection showed no evidence of recurrence and had a relatively satisfactory palpebral appearance. In the other 2 patients (cases 5 and 6), oral steroids and antibiotics were immediately administered combined with physiotherapy after the biopsies. The latest follow-up MR imaging showed complete resolution in case 5 (Figs 3A, -*C*) and slight improvement in case 6.

Discussion

Periorbital lipogranuloma has characteristic histologic features—that is, variable-sized microcysts containing lipid materials with a surrounding prominent histiocytic, lymphocytic, and foreign body–type multinucleated giant cell reaction with areas of fibrosis and fat necrosis. Immunohistochemistry is also very helpful, with positivity for CD68 highlighting the histiocytic cellular component of foreign-body reaction.[11,12]

The mechanism of the formation of periorbital lipogranuloma after ESS is not yet fully explained in the literature, to our knowledge. Two theories have been proposed to explain it.[3,5,8,13] The first theory suggests that the initiating factor is due to the placement of ointment-based gauze for control of bleeding during ESS. The exogenous lipid then migrates to the anterior orbit and eyelids through hemorrhage as a result of packing pressure. The blood subsequently emulsifies the ointment and distributes it to the surrounding tissues. After the blood has been absorbed, tiny droplets of the ointment product remain and cause a foreign-body reaction that elicits formation of the lipogranuloma.[4,6]

The second theory proposes that lipogranuloma formation is the result of a combination of factors in some patients, not using ointment products, including an injury to the lamina papyracea, which provides a pathway into the orbit, and postoperative hemorrhage and hematoma formation within the orbital cavity. This compression of hemorrhage and hematoma formation may cause necrosis of orbital fat tissue and accumulation of free extracellular fat droplets. The fat droplets then lead to a secondary granulomatous reaction and the formation of lipogranuloma.[5] On the basis of the literature[3,8] and the present cases, we speculate that the formation of periorbital lipogranuloma after ESS may be related to many factors, including injury of the lamina papyracea, amount of bleeding, packing gauze with ointment concentrations, lacrimal duct penetration, and idiosyncratic host response.

In the literature, onset ranges from several weeks to years after ESS.[5,6,8] In this series, the mean time was 6 months (range, 1–25 months) from ESS to presentation of a palpable mass of the eyelid. Patients with periorbital lipogranuloma typically present with eyelid swelling associated with multiple nodules several months or years after ESS. Firm, ill-circumscribed, and painless masses in the eyelid are often detected on clinical examination. The lesions generally do not cause visual acuity decrease, ocular motility limitation, or proptosis. Some patients with periorbital lipogranuloma have a history of eye pain, swelling, proptosis, and periorbital ecchymosis immediately after ESS. After medication, as swelling gradually subsides, these patients develop a slowly growing irregular mass of the eyelid.

On the basis of our cases and the literature,[5,8] the CT and MR imaging characteristics of periorbital lipogranuloma are specific. On nonenhanced CT, periorbital lipogranuloma usually shows inhomogeneous isoattenuation relative to adjacent extraocular muscles with multiple locules of fat deposits around the eyelid. Some patients had incontinuity of the lamina papyracea. The postoperative appearance of the sinonasal cavity after ESS is clearly noted on CT as well. Periorbital lipogranuloma is generally heterogeneously isointense compared with adjacent extraocular muscle on both T1- and T2-weighted images, with moderate inhomogeneous enhancement after contrast administration. Multiple, speckled, or nodular well-defined foci are scattered within these lesions, which demonstrate high signal on T1-weighted images and intermediate signal on T2-weighted images and become hypointense after using a fat-suppression technique, corresponding to fatty tissue. These imaging findings are indicative of a fat lesion with an inflammatory tissue reaction.

DCE MR imaging can provide information related to lesion perfusion, microvascular permeability, and volume of the extracellular space, information that may help to diagnose some lesions and predict their biologic behavior.[9,10] For example, a TIC on DCE MR imaging may provide valuable information in differentiating benign from malignant lesions. The TICs of our 6 patients in the present study showed a persistent pattern (type I), which suggests a benign lesion. Histologically, this may be related to inflammatory granuloma areas. To the best of our knowledge, there have been no previously documented reports regarding DCE MR imaging of periorbital lipogranuloma in the literature.

Owing to the eyelid swelling, patients often see an ophthalmologist several weeks or months after ESS. Unfortunately, most ophthalmologists seem to be unaware of the fact that periorbital lipogranuloma can be a complication of ESS, thus the causal relationship is often overlooked, and this omission eventually leads to a delay in diagnosis. The lesions usually require a surgical excision.

Conclusions

The clinical diagnosis of periorbital lipogranuloma can be difficult in the absence of clinical history or without knowledge of the ESS complications; however, imaging may give an important clue to the diagnosis of the disease entity. Recognition of the characteristic imaging appearance of periorbital lipogranuloma, multiple locules of fat deposits within an irregular-shaped soft-tissue mass in the eyelid, can help physicians make the correct diagnosis and select the appropriate management.

References

1. Bhatti MT, Stankiewicz JA. **Ophthalmic complications of endoscopic sinus surgery**. *Surv Ophthalmol* 2003;48:389–402
2. Han JK, Higgins TS. **Management of orbital complications in endoscopic sinus surgery.** *Curr Opin Otolaryngol Head Neck Surg* 2010;18:32–36
3. Witschel H, Geiger K. **Paraffin induced sclerosing lipogranuloma of eyelids and anterior orbit following endonasal sinus surgery.** *Br J Ophthalmol* 1994;78:61–65
4. Hintschich CR, Beyer-Machule CK, Stefani FH. **Paraffinoma of the periorbit – a challenge for the oculoplastic surgeon.** *Ophthal Plast Recontr Surg* 1995;11:39–43
5. Rosner M, Kurtz S, Shelah M, et al. **Orbital lipogranuloma after sinus surgery.** *Eur J Ophthalmol* 2000;10:183–86
6. Keefe MA, Bloom DC, Keefe KS, et al. **Orbital paraffinoma as a complication of endoscopic sinus surgery.** *Otolaryngol Head Neck Surg* 2002;127:575–77
7. Merkur AB, Jardeleza MS, Iliff NT, et al. **Periocular petrolatum.** *Ophthal Plast Reconstr Surg* 2005;21:23–31
8. Hasegawa T, Yukawa K, Suzuki M, et al. **A case of eyelid paraffinoma that developed after endoscopic sinus surgery.** *Auris Nasus Larynax* 2011;38:538–42
9. Yabuuchi H, Fukuya T, Tajima T, et al. **Salivary gland tumors: diagnostic value of gadolinium-enhanced dynamic MR imaging with histopathologic correlation.** *Radiology* 2003;226:345–54
10. Hisatomi M, Asaumi J, Yanagi Y, et al. **Diagnostic value of dynamic contrast-enhanced MRI in the salivary gland tumors.** *Oral Oncol* 2007;43:940–47
11. Sa HS, Woo KI, Suh YL, et al. **Periorbital lipogranuloma: a previously unknown complication of autologous fat injections for facial augmentation.** *Br J Ophthalmol* 2011;95:1259–63
12. Abel AD, Carlson JA, Bakri S, et al. **Sclerosing lipogranuloma of the orbit after periocular steroid injection.** *Ophthalmology* 2003;110:1841–45
13. Bassichis BA, Thomas JR. **Foreign-body inclusion cyst presenting on the lateral nasal sidewall 1 year after rhinoplasty.** *Arch Facial Plast Surg* 2003;5:530–32